Revision 1 of "A comparative analysis of the mechanical behavior of carbon dioxide and methane hydrate-bearing sediments"

Masayuki Hyodo,[1] Yanghui Li,[1,2,]* Jun Yoneda,[3] Yukio Nakata,[1] Norimasa Yoshimoto,[1] Shintaro Kajiyama,[1] Akira Nishimura,[1] and Yongchen Song[2]

[1]Dept. of Civil and Environmental Engineering, Yamaguchi University, Tokiwadai 2-16-1, Ube, Japan.

[2]Key Lab. of Ocean Energy Utilization and Energy Conservation of Ministry of Education, Dalian University of Technology, Dalian, China.

[3]The National Institute of Advanced Industrial Science and Technology, Tsukuba, Ibaraki Japan.

Abstract

Understanding the mechanical behaviors of carbon dioxide/methane hydrate-bearing sediments is essential for assessing the feasibility of CO_2 displacement recovery methods to produce methane from hydrate reservoirs. In this study, a series of drained triaxial compression tests were conducted on synthetic carbon dioxide hydrate-bearing sediments under various conditions. A comparative analysis was also made between carbon dioxide and methane hydrate-bearing sediments. The stress-strain curves, shear strength and the effects of hydrate saturation, effective confining stress, and temperature on the mechanical behaviors were investigated. Our experimental results indicate that the newly formed carbon dioxide hydrate would keep the reservoir mechanically stable when CH_4-CO_2 gas exchange took place in a relatively short period of time and spatially well distributed in the pore space. And experiments of CO_2 injection in

* E-mail: li.yanghui@mail.dlut.edu.cn

methane hydrate-bearing sediments are necessary to confirm this hypothesis.

Keywords: carbon dioxide hydrate; mechanical behavior; CH_4-CO_2 replacement technology; triaxial tests

1. Introduction

There is a large amount of natural gas that exists in continental margins and permafrost regions in the form of methane hydrate around the world (Kvenvolden 1988; Kvenvolden et al. 1993). This amount far exceeds all conventional fossil fuels on earth and could provide for the energy demands of human beings well into the next century (Boswell and Collett 2011). Methane in hydrates is very dispersed in the earth upper crust and that hydrate-bearing sands are the most economically viable reservoirs for gas production from hydrate-bearing sediments. JOGMEC (Japan Oil, Gas and Metals National Corporation) successfully extracted natural gas from hydrate layers in a first of its kind offshore production test on March 12, 2013; representing a step forward in the research and development of methane hydrate as a potential energy resource. However, it is still an enormous challenge for current technology (Boswell 2009; Glasby 2003; Lee and Holder 2001; Ning et al. 2012).

Conventional methods for the production of natural gas hydrate include thermal stimulation, depressurization, and chemical injection (Kamath et al. 1991; Sung et al.

(DOI will not work until issue is live.) DOI: http://dx.doi.org/10.2138/am.2014.4620

2002; Tang et al. 2005). Ohgaki et al. (1994, 1996) first introduced the concept of exchanging CO_2 with CH_4 in natural gas hydrate reservoirs; a concept which has attracted more and more attention due to two secondary benefits: mechanical stability and mitigating global warming. Nakazono et al. (2008) proposed a new method of generating carbon dioxide hydrate in the sediments on top of methane hydrate layers to build artificial roofs for the prevention of landslides and to inhibit the methane dissociated in production from diffusing to the sea. However, there are many uncertainties in this production process, especially related to ground deformation. The evaluation of mechanical behavior in methane and carbon dioxide hydrate-bearing sediments will affect the stability of production wellbores and hydrate reservoirs (Espinoza and Santamarina 2011). Thus, in order to assess the feasibility of the CO_2 displacement recovery method and the long-term stability of the hydrate reservoir, the mechanical behavior of carbon dioxide and methane hydrate-bearing sediments should be clearly investigated.

The thermodynamic feasibility of CH_4-CO_2 replacement reaction is well studied, and the results indicate that the gas exchange technology is plausible (Hirohama et al. 1996; Kvamme et al. 2007; Lee et al. 2003; McGrail et al. 2007). However, the mechanical behavior of carbon dioxide hydrate-bearing sediments and the difference with that of methane hydrate-bearing sediments are rarely investigated. Uchida and Kawabata (1997) studied the mechanical properties of the liquid CO_2-water-CO_2-hydrate system for the assessment of the applicability of deep sea sequestering of CO_2. Both the interfacial tensions in these phases and the strength of the carbon dioxide hydrate film were measured. Espinoza and Santamarina (2011) monitored P-wave velocity in hydrate-bearing sand during CH_4-CO_2 replacement. The results showed that CH_4-CO_2 replacement occurs without a loss of stiffness in the granular medium, implying that CH_4-CO_2 replacement can remain mechanically stable during and after CH_4 gas production. Wu and Grozic (2008) studied the isotropic undrained dissociation behavior of carbon dioxide hydrate-bearing sands. The study demonstrated that the dissociation of even a small amount of gas hydrates could lead to soil failure. Ordonez and Grozic (2011) investigated the effects of carbon dioxide hydrates on P-wave velocity and shear strength in Ottawa sand. The shear strength and stiffness increased in the presence of gas hydrates; friction angle was unaffected while an apparent increase in cohesion was observed. Many researchers studied the mechanical behaviors of methane hydrate-bearing sediments (Hyodo et al. 2005, 2013; Masui et al. 2005; Miyazaki et al. 2011a; Li et al. 2011, 2012a, 2012b, 2012c; Winters et al. 2007; Yoneda et al. 2010). The results indicated that the failure strength and stiffness of methane hydrate-bearing sediments increased with increasing hydrate saturation, effective confining stress and back pressure, while decreased with increasing temperature and porosity.

In this study, a series of triaxial compression tests were conducted in order to investigate the mechanical behavior of carbon dioxide hydrate-bearing sediments under various conditions. And the results were compared to that of methane hydrate-bearing sediments which come from the literatures (Hyodo et al. 2013; Masui et al. 2008; Miyazaki et al. 2011a).

2. Experimental Details

A temperature-controlled high pressure triaxial testing apparatus was developed to study the mechanical behavior of gas hydrates and their interaction with soil and rock. It can reproduce the *in situ* conditions of gas hydrate reservoirs, allowing for research into the formation and dissociation processes of gas hydrates in deep sea beds. The schematic diagram and details of this apparatus have been introduced in our earlier studies (Hyodo et al. 2013).

A brief description of the test procedure is shown in Fig.1. Specimen preparation for these tests involved reconstituting Toyoura sand using a moist tamping method with a specimen diameter of 30mm and height of 60mm, resulting in a relative density of 90%, and porosity of around 0.4. In order to make the specimen stand by itself, the specimen was tightly sealed and placed in a freezer. A butyl rubber membrane was used to cover the specimens during shear tests.

Once the triaxial cell was assembled, the cell fluid (temperature of -1℃) was added, and the confining pressure increased to 0.2 MPa. Next, CO_2 was injected into the specimen and gradually increased to 3.5 MPa, the confining pressure was kept 0.2 MPa higher than the pore pressure and the temperature of cell fluid turned to 5℃. Such conditions were held constant for 24h to generate carbon dioxide hydrate. We considered that the water was fully converted to hydrate when there was no obvious volume change in the upper and lower syringe pumps connected to the top and bottom of the specimen (Hyodo et al. 2013). From Fig.1, it can be observed that the carbon dioxide hydrate formed in the study was outside the methane hydrate phase stability field. In such conditions, the methane hydrate would dissociate just as in the situation of CH_4-CO_2 replacement in hydrate.

After the hydrate was generated, pure water under constant pressure (3.5 MPa) was injected into the specimen to replace the residual CO_2 gas in the pore spaces. Although some dissociation of hydrate was anticipated during injection, the exact value of hydrate saturation was measured after the test by colleting the dissociated CO_2 gas using a gas flow meter, and the result was almost the same as we expected. It indicated that the dissociation of hydrate is very little due to the injection of pure water. Then, back pressure and confining pressure were applied, the temperature was adjusted to the desired condition. While keeping the pressure constant, isotropic consolidation was carried out until the desired effective stress was reached, and then the shear test would be conducted. The axial strain rate was 0.1%/min.

The regions in which methane hydrate is potentially stable commonly from a few hundred to a thousand meters below the seafloor (normally with a range of temperature, back pressure, effective confining stress, and saturation of around 0-15℃, 3-20 MPa, 0-10 MPa and 0-75%, respectively). In this study, triaxial compression tests were conducted using the conditions shown in Table 1.

3. Results and Discussion

3.1 Stress-strain curves

The stress-strain curve is unique for each material and is found by recording the amount of deformation (strain) at distinct intervals of compressive loading (stress). These curves reveal many of the properties of a material, which can be used to establish a constitutive model or strength criteria. It is essential to study the stress-strain curves in order to clearly understand the deformation behavior of a gas hydrate reservoir.

Fig.2 shows the deviatoric stress, axial strain and volumetric strain relations of carbon dioxide and methane hydrate-bearing sediments under various hydrate saturations and constant effective confining stress of 5 MPa and temperature of 5℃. We observe that the stress-strain curves of carbon dioxide and methane hydrate-bearing sediments both occur as a hyperbolic tangent functions under such conditions. The deviatoric stress increases almost linearly with increasing axial strain when the axial strain is less than 0.5-1% with a little plastic strain. With the further increase of axial strain, the deviatoric stress continues to increase; however, the stress increment ratio gradually decreases.

From Fig.2, the stress-strain curve can be divided into three stages: quasi-elastic stage, the hardening stage and the yielding stage. For carbon dioxide hydrate-bearing specimens, the quasi-elastic and hardening stage were observed. A significant strain hardening behavior was observed until the end of compression. The shapes of the stress-strain curves were similar to that of Toyoura sand. For methane hydrate-bearing specimens, all three stages were observed. The strain hardening stage finished at the axial strain of 4%-5%, followed by a yielding stage with a slight hardening. The deviatoric stress increased more rapidly with axial strain than that of carbon dioxide hydrate-bearing specimens at the beginning of the test, while reaching the same ultimate value of strength at the end of the test. Thus, the initial stiffness of the methane hydrate-bearing specimens was higher than that of carbon dioxide hydrate-bearing specimens under similar hydrate saturation, but the failure strength was almost the same. When a strain hardening hydrate-bearing sediment under a constant loading of failure strength, a deviatoric stress increment is still required to produce the axial strain. while a strain-hardening plus yielding hydrate-bearing sediment under a loading of failure strength, the specimen is able to continue deforming under even a tiny stress increment, which implies that the specimen loses its ability to resist deformation and is destroyed. In this study, the failure strength was defined as the peak value of deviatoric stress during the compression until the axial strain reached 15%.

As referred to in the literature, the stress-strain curves of gas hydrate-bearing sediments or natural hydrate cores may show a softening behavior during the compression (Masui et al. 2008; Miyazaki et al. 2011a; Ordonez and Grozic 2011). The stress-strain curves vary with test conditions, and it is believed that the various preparation conditions for the methane hydrate-bearing specimens led to such differences.

The volumetric strain of carbon dioxide hydrate-bearing specimens showed shear contraction behavior during compression under various hydrate saturations. While the volumetric strain of methane hydrate-bearing specimens presented an obviously different behavior to that of carbon dioxide hydrate-bearing specimens. At 41.9% methane hydrate saturation, the volumetric strain showed a shear dilatation behavior.

The specimen was compacted first, and then dilated gradually until the end of the experiment. At 35.1% methane hydrate saturation, the volumetric strain was less than that of the carbon dioxide hydrate-bearing specimen at the same axial strain.

Fig.3 shows deviatoric stress differences relative to the Toyoura sand for various hydrate saturations at a constant effective confining stress of 5 MPa and temperature of 5 ℃. Both the deviatoric stress increment of carbon dioxide and methane hydrate-bearing specimens increase almost linearly with axial strain at the beginning of the compression. For carbon dioxide hydrate-bearing specimens, the deviatoric stress increment gradually increases without any significant peak value and remains constant until the end of the test. For methane hydrate-bearing specimens, the deviatoric stress increment reaches a peak value at the axial strain of 1%-3%, then follows a decline until the end. Although the deviatoric stress increments were much higher than that of carbon dioxide hydrate-bearing specimens, the final residual increment was almost the same under various hydrate saturations.

3.2 The influence of hydrate saturation

The influence of hydrate saturation on methane hydrate-bearing sediments has been well studied in the literature (Hyodo et al. 2013; Miyazaki et al. 2011a; Waite et al. 2009; Winters et al. 2004): The larger the methane hydrate saturation, the larger the strength and the more apparent the dilatation behavior. The existence of hydrate will also affect the stress-strain curve of the specimen.

In Fig.2, we can also observe that the mechanical properties of all samples vary with carbon dioxide hydrate saturation. The carbon dioxide hydrate-bearing specimens showed compressive volume change and strain hardening behavior at effective confining stress of 5 MPa. A marked increase of the initial stiffness and failure strength occurred with the increase of carbon dioxide hydrate saturation, which was similar to that observed in the methane hydrate-bearing specimens. However, the volumetric strain and the shape of stress-strain curves for the carbon dioxide hydrate-bearing samples changed very little as the hydrate saturation increased. This is much different from that of methane hydrate, whose volumetric strain changes from compressive to dilative and the stress-strain curves changes from strain hardening behavior to strain softening behavior as hydrate saturation increases.

In Fig.3, it is observed that the deviatoric stress increment of the specimen with 44.9% carbon dioxide hydrate saturation was larger than that of the specimen with 32.7% carbon dioxide hydrate saturation at the same axial strain. It is believed that the strength increment is affected by cementation (Masui et al. 2005) and the bulk density of the specimen. For higher hydrate saturations, the cementation effect between sand particles is stronger and the bulk density is higher, which causes an enhancement of strength.

Fig.4 shows the failure strength plotted against the hydrate saturation for carbon dioxide hydrate, methane hydrate and natural hydrate cores as well as for the sand skeleton. The failure strength of carbon dioxide hydrate-bearing specimens was close to that of methane hydrate-bearing specimens under similar test conditions. Also, the failure strength of synthetic methane hydrate-bearing specimens was almost the same to that of natural hydrate cores. The failure strength increases with hydrate saturation under various effective confining stresses, which can be well regressed by exponential functions. This result indicates that the large-strain shear strength of carbon dioxide hydrate-bearing sediments is comparable to the one of methane hydrate-bearing sediments. Thus, if CH_4-CO_2 gas exchange took place in a relatively short period of time and spatially well distributed in the pore space, then, acting deviatoric stresses on the methane hydrate-bearing sediments could be resisted by the newly formed carbon dioxide hydrate keeping the reservoir mechanically stable.

3.3 The influence of effective confining stress

According to the literature, the mechanical properties of sands are dependent on the effective confining stress (Alkire and Andersland 1973; Ma et al. 1999; Miyazaki et al. 2011b; Yang et al. 2010). Stress-strain curves should change from strain softening to strain hardening with increasing effective confining stress.

Fig.5 shows the deviatoric stress, axial strain and volumetric strain relationships of carbon dioxide hydrate-bearing specimens under different effective confining stresses (σ_c'= 1 MPa, 2 MPa, 5 MPa) with constant back pressure, temperature and broadly similar hydrate saturations. For an effective confining stress σ_c'= 1 MPa, the stress-strain curve showed strain softening behavior. The volumetric strain was compressive at first, then turned dilative until the end of the experiment. The curves were clearly dependent on the effective confining stress as in the case of other geological materials; under higher effective confining stresses, the specimens had a larger strength and greater stiffness and showed increasing amounts of strain hardening behavior. As showed for effective confining stress σ_c'= 5 MPa, no significant peak value was presented and volumetric strain became compressive. Similar testing results can be found in the studies of Hyodo et al. (2013) and Miyazaki et al. (2011a).

Fig.6 shows the failure strength of carbon dioxide hydrate-bearing specimens plotted against the effective confining stress. Similar testing results from Miyazaki et al. (2011a) and Hyodo et al. (2013) are also plotted in Fig.6. The failure strength of both carbon dioxide hydrate and methane hydrate-bearing specimens increases markedly with effective confining stress. This increasing effective confining stress restricts the growth of fractures, which may increase the inter-particle coordination and frictional resistance, as noted by Yun et al. (2007). They studied the confining stress dependence on the strength of THF hydrate-bearing sediments and noted that a higher effective confining stress led to higher inter-particle coordination prior to hydrate formation, and hence a higher strength. Also note that the failure strength of methane hydrate-bearing sediments used in the study of Miyazaki et al. (2011a) was higher than that of carbon dioxide hydrate-bearing sediments at similar saturations, which is seemingly against the results obtained in section 3.2. In this study, a cylindrical-shaped load cell was set up inside the cell to eliminate the influence of piston friction which would be very large under high cell pressures (Hyodo et al. 2013). While Miyazaki et al. (2011a) set up the load cell outside the cell, the strength results included the friction of piston and showed larger values. Also the porosity (37.8%) of the specimens Miyazaki et al. (2011a) used is smaller than that of ours, which should present higher failure strength.

3.4 The influence of temperature

Figs. 7 and 8 show the influence of temperature on the mechanical properties of carbon dioxide hydrate-bearing specimens. The initial stiffness and failure strength are dependent on the temperature. The temperature drop led to the increase of initial stiffness and failure strength. The volumetric strain showed little temperature dependence. Similar results were found for methane hydrate-bearing specimens (Hyodo et al. 2013), as shown in Fig.8.

These results confirm the conclusions of earlier hydrate research where the lower the temperature, the higher the strength (Durham et al. 2003). It is believed that hydrate is more thermodynamically stable at lower temperatures, which leads to an enhancement of intermolecular forces and makes it more difficult to mechanically fail.

3.5 Shear strength

Shear strength is a combination of the cohesion and internal friction angle, which includes resistance to sliding between particles, particle rearrangement, and particle crushing. These two contributions to shear strength are captured in the Mohr-Coulomb failure criterion. Cohesion reflects the combination of physical-chemical forces between particles, such as cementation between sand grains. The internal friction angle describes the effective stress-dependent frictional resistance, including surface friction force and interlocking force of particles. However, the cohesion and internal friction angle are always affected by experimental methods. In this study, the shear strength was described as a function of effective cohesion (c') and effective internal friction angle (φ'), as shown in Fig.9. It can be clearly observed that the effective cohesion and internal friction angle of methane hydrate-bearing sediments raise 0.11MPa and 2.8° as the hydrate saturation increased from 0% to 43-48% respectively; and those of carbon dioxide hydrate-bearing sediments raise 0.06MPa and 0.2° as the hydrate saturation increased from 0% to 23%-26% respectively.

Ordonez and Grozic (2011) found a friction angle of 45° for both Ottawa sand specimens (with and without carbon dioxide hydrates), the moist sand specimens exhibited no cohesion, but the hydrate-bearing specimens developed an apparent cohesion of approximately 0.14MPa. They interpreted this cohesion for hydrate-bearing specimens as the result of cementation of the sand grains, which resulted in an increase in strength. Yoneda et al. (2013) conducted plane strain compression tests on pure Toyoura sand and methane hydrate-bearing sediments with localized deformation measurement, which indicated that the friction angle of methane hydrate-bearing sediments is greater than that of host sand. Although the shear strength, cohesion and internal friction angle are known to vary with host materials, we confirm that the effective cohesion increases with increasing hydrate saturation, and that the effective internal friction angle shows little dependency on the hydrate saturation. It is believed that the presence of hydrate will cement unconsolidated sediments (Waite et al. 2004), which will enhance the cementing force between sand grains and result in an increase in effective cohesion.

4. Implications

Our main finding indicates that the newly formed carbon dioxide hydrate-bearing sediments would keep the reservoir mechanically stable when CH_4-CO_2 gas exchange took place in a relatively short period of time and spatially well distributed in the pore space. This is intriguing because it verifies the possibility of a new kind of methane hydrate mining and a potential carbon dioxide storage method. However, experiments of CO_2 injection in methane hydrate-bearing sediments are necessary to confirm this hypothesis in further studies. Also, the obtained mechanical parameters are expected to be used to fully understand the deformation of hydrate-bearing layers and to establish a constitutive model in future studies, which is important to assess the long-term stability of methane hydrate-bearing reservoirs.

5. Acknowledgments

This work was supported by a Grant-in Aid for scientific research (A) No.20246080 of Japan Society for the Promotion of Science. The second author was supported to stay in Yamaguchi University as a research student by a grant from the Major National S&T Program (No. 2011ZX05026-004), and a scholarship under the State Scholarship Fund of China Scholarship Council. The authors would like to express their sincere thanks to their supports.

References:

Alkire, D.B., and Andersland, B.O. (1973) The effect of confining pressure on the mechanical properties of sand-ice materials. Journal of Glaciology, 12(66), 469-481.

Boswell, R. (2009) Is gas hydrate energy within reach? Science, 325(5943), 957-958.

Boswell, R., and Collett, T.S. (2011), Current perspectives on gas hydrate resources, Energy & Environmental Science, 4(4), 1206-1215.

Durham, W.B., Kirby S.H., Stern, L.A. and Zhang, W. (2003) The strength and rheology of methane clathrate hydrate. Journal of Geophysical Research, 108(B4), 2182.

Espinoza, D.N., and Santamarina, J.C. (2011) P-wave monitoring of hydrate-bearing sand during CH_4-CO_2 replacement. International Journal of Greenhouse Gas Control, 5(4), 1031-1038.

Glasby, G.P. (2003) Potential impact on climate of the exploitation of methane hydrate deposits offshore. Marine and Petroleum Geology, 20(2), 163-175.

Hirohama, S., Shimoyama, Y., Wakabayashi, A., Tatsuta, S., and Nishida, N. (1996) Conversion of CH_4-hydrate to CO_2-hydrate in liquid CO_2. Journal Of Chemical Engineering Of Japan, 29(6), 1014-1220.

Hyodo, M., Nakata, Y., Yoshimoto, N., and Ebinuma, T. (2005) Basic research on the mechanical behavior of methane hydrate-sediments mixture. Soils and Foundations, 45(1), 75-85.

Hyodo, M., Yoneda, J., Yoshimoto, N., and Nakata, Y. (2013) Mechanical and dissociation properties of methane hydrate-bearing sand in deep seabed. Soils and Foundations, 53(2), 299-314.

Kamath, V.A., Mutalik, P.N., Sira, J.H., and Patil, S.L. (1991) Experimental study of brine injection depressurization of gas hydrates dissociation of gas hydrates. SPE Formation Evaluation, 6(4), 477-484.

Kvamme, B., Graue, A., Buanes, T., Kuznetsova, T., and Ersland, G. (2007) Storage of CO_2 in natural gas hydrate reservoirs and the effect of hydrate as an extra sealing in cold aquifers. International Journal of Greenhouse Gas Control, 236-246.

Kvenvolden, K.A. (1988) Methane hydrate-A major reservoir of carbon in the shallow geosphere? Chemical Geology, 71(1-3), 41-51.

Kvenvolden, K.A., Ginsburg, G.D., and Soloviev, V.A. (1993) Worldwide distribution of subaquatic gas hydrates. Geo-Marine Letters, 13(1), 32-40.

Lee, H., Seo, Y., Seo, Y., Moudrakovski, I.L., and Ripmeester, J.A. (2003) Recovering methane from solid methane hydrate with carbon dioxide. Angewandte Chemie, 115(41), 5202-5205.

Lee, S.Y., and Holder, G.D. (2001) Methane hydrates potential as a future energy source. Fuel Processing Technology, 71(1-3), 181-186.

Li, Y., Song, Y., Yu, F., Liu, W., and Zhao, J. (2011) Experimental study on mechanical properties of gas hydrate-bearing sediments using kaolin clay. China Ocean Engineering, 25(1), 113-122.

Li, Y., Song, Y., Liu, W., Yu, F., Wang, R., and Nie, X. (2012a) Analysis of mechanical properties and strength criteria of methane hydrate-bearing sediments. International Journal of Offshore and Polar Engineering, 22(4), 290-296.

Li, Y., Song, Y., Liu, W., and Yu, F. (2012b) Experimental research on the mechanical properties of methane hydrate-ice mixtures. Energies, 5(2), 181-192.

Li, Y., Zhao, H., Yu, F., Song, Y., Liu, W., Li, Q., and Yao, A.H. (2012c) Investigation of the stress-strain and strength behavior of ice containing methane hydrate. Journal of Cold Regions Engineering, 26(4), 149-159.

Ma, W., Wu, Z., Zhang, L., and Chang, X. (1999) Analyses of process on the strength decrease in frozen soils under high confining pressures. Cold Regions Science and Technology, 29(1), 1-7.

Masui, A., Haneda, H., Ogata, Y., and Aoki, K. (2005) Effects of methane hydrate formation on shear strength of synthetic methane hydrate sediments. Proceedings of the Fifteenth (2005) International Offshore and Polar Engineering Conference, 1, 364-369.

Masui, A., Miyazaki, K., Haneda, H., Ogata, Y., and Aoki, K. (2008) Mechanical characteristics of natural and artificial gas hydrate bearing sediments. Proceedings of the 6th International Conference on Gas Hydrates (ICGH 2008), Vancouver, British Columbia, CANADA.

McGrail, B.P., Schaef, H.T., White, M.D., Zhu, T., Kulkami, A.S., Hunter, R.B., Patil, S.L., Owen, A.T., and Martin, P.F. (2007) Using carbon dioxide to enhance recovery of methane from gas hydrate reservoirs: final summary report. Pacific Northwest National Laboratory operated by Battelle Memorial Institute for the U.S. Department of Energy, Oak Ridge, TN.

Miyazaki, K., Masui, A., Sakamoto, Y., Aoki, K., Tenma, N., and Yamaguchi, T. (2011a) Triaxial compressive properties of artificial methane-hydrate-bearing sediment. Journal of Geophysical Research-Solid Earth, 116(B06102).

Miyazaki, K., Tenma, N., Aoki, K., Sakamoto, Y., and Yamaguchi, T. (2011b) Effects of confining pressure on mechanical properties of artificial methane-hydrate-bearing sediment in triaxial compression test. International Journal of Offshore and Polar Engineering, 21(2), 148-154.

Nakazono, M., Jiang, Y., and Tanabashi, Y. (2008) Study on the use possibility of carbon dioxide hydrate in methane hydrate dissolution. The fifth China-Japan Joint Seminar for the Graduate Students in Civil Engineering, Shanghai, China.

Ning, F., Yu, Y., Kjelstrup, S., Vlugt, T.J.H., and Glavatskiy, K. (2012) Mechanical properties of clathrate hydrates: status and perspectives. Energy & Environmental Science, 5(5), 6779-6795.

Ohgaki, K., Takano, K., Sangawa, H., Matsubara, T., and Nakano, S. (1996) Methane exploitation by carbon dioxide from gas hydrates-phase equilibria for CO_2-CH_4 mixed hydrate system. Journal Of Chemical Engineering Of Japan, 29(3), 478-483.

Ohgaki, K., Takano, K., and Moritoki, M. (1994) Exploitation of CH_4 hydrates under the Nankai Trough in combination with CO_2 storage. Kagaku Kogaku Ronbunshu, 20(1), 121-123.

Ordonez, C., and Grozic, J.L.H. (2011) Strength and compressional wave velocity variation in carbon dioxide hydrate bearing Ottawa sand. 2011 Pan-Am CGS Geotechnical Conference, Toronto, Canada.

Sung, W., Lee, H., Lee, H., and Lee, C. (2002) Numerical study for production performances of a methane hydrate reservoir stimulated by inhibitor injection. Energy sources, 24(6), 499-512.

Tang, L.G., Xiao, R., Huang, C., Feng, Z.P., and Fan, S.S. (2005) Experimental investigation of production behavior of gas hydrate under thermal stimulation in unconsolidated sediment. Energy & Fuels, 19(6), 2402-2407.

Uchida, T., and Kawabata, J. (1997) Measurements of mechanical properties of the liquid CO2-water-CO2-hydrate system. Energy, 22(2-3), 357-361.

Waite, W.F., Santamarina, J.C., Cortes, D.D., Dugan, B., Espinoza, D.N., Germaine, J., Jang, J., Jung, J.W., Kneafsey, T.J., Shin, H., Soga, K., Winters, W.J., and Yun, T.S. (2009) Physical properties of gas hydrate-bearing sediments. Reviews of Geophysics, 47(RG4003).

Waite, W.F., Winters, W.J., and Mason, D.H. (2004) Methane hydrate formation in partially water-saturated Ottawa sand. American Mineralogist, 89(8-9), 1202-1207.

Winters, W.J., Pecher, I.A., Waite, W.F., and Mason, D.H. (2004) Physical properties and rock physics models of sediment containing natural and laboratory-formed methane gas hydrate. American Mineralogist, 89(8-9), 1221-1227.

Winters W.J., Waite W.F., Mason D.H., Gilbert L.Y., Pecher I.A. (2007) Methane gas hydrate effect on sediment acoustic and strength properties. Journal of Petroleum Science and Engineering, 56(1-3): 127-135.

Wu, L., and Grozic, J.L.H. (2008) Laboratory analysis of carbon dioxide hydrate-bearing sands. Journal of Geotechnical & Geoenvironmental Engineering, 134(4), 547-550.

Yang, Y., Lai, Y., and Li, J. (2010) Laboratory investigation on the strength characteristic of frozen sand considering effect of confining pressure. Cold Regions Science and Technology, 60(3), 245-250.

Yoneda, J., Hyodo, M., Nakata, Y., Yoshimoto, N. (2010) Triaxial shear characteristics of methane hydrate-bearing sediment in the deep seabed, Journal of JSCE (III): Geotechnical Engineering, 66(4): 742-756.

Yoneda, J., Hyodo, M., Yoshimoto, N., Nakata, Y., Kato, A. (2013) Development of high pressure low temperature plane strain testing apparatus for methane hydrate-bearing sand, Soils and Foundations, in press.

Yun, T.S., Santamarina, J.C., and Ruppel, C. (2007) Mechanical properties of sand, silt, and clay containing tetrahydrofuran hydrate. Journal of Geophysical Research, 112(B04106).

Figure captions

Fig.1 The pressure/temperature conditions during the preparation of carbon dioxide hydrate-bearing specimens.

Fig.2 The stress-strain curves and volumetric strain of carbon dioxide and methane hydrate-bearing sediments.

Fig.3 The deviatoric stress difference relative to the host Toyoura sand for various hydrate saturations under different hydrate saturation conditions.

Fig.4 The influence of hydrate saturation on the failure strength of synthetic carbon dioxide hydrate, methane hydrate and natural hydrate cores.

Fig.5 The influence of effective confining stress on the stress-strain curves and volumetric strain of carbon dioxide hydrate-bearing specimens.

Fig.6 The influence of effective confining stress on the failure strength of carbon dioxide and methane hydrate-bearing specimens.

Fig.7 The influence of temperature on the stress-strain curves and volumetric strain of carbon dioxide hydrate-bearing specimens.

Fig.8 The influence of temperature on the failure strength of carbon dioxide and methane hydrate-bearing specimens.

Fig.9 Shear strength and Mohr's circles of hydrate-bearing specimens.

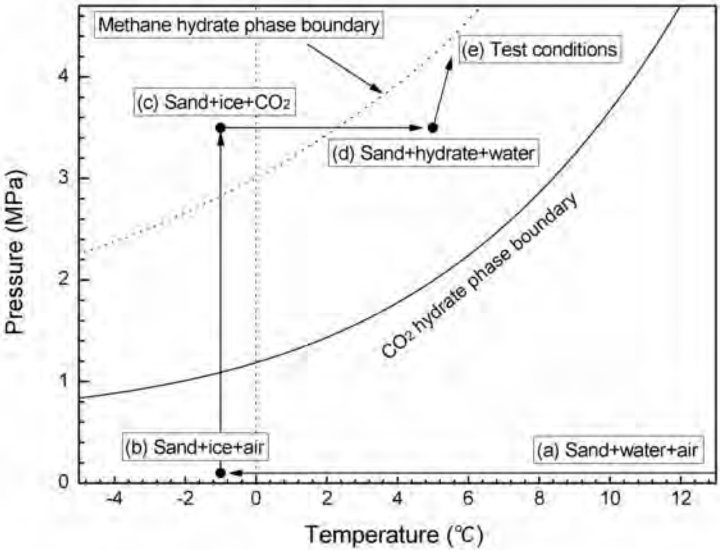

Methane hydrate phase boundary
(e) Test conditions
(c) Sand+ice+CO2
(d) Sand+hydrate+water
CO2 hydrate phase boundary
(b) Sand+ice+air
(a) Sand+water+air
Pressure (MPa)
Temperature (℃)
0
1
2
3
4
-4
-2
0
2
4
6
8
10
12

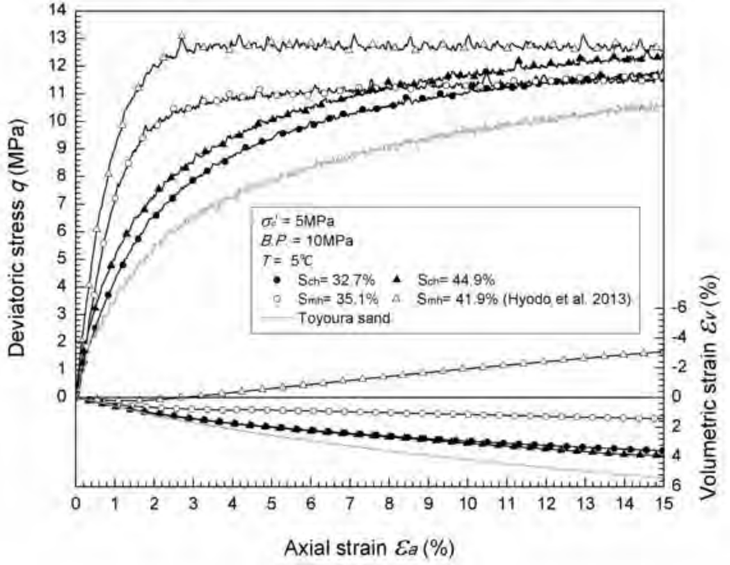

Deviatoric stress q (MPa)
Volumetric strain εv (%)
Axial strain εa (%)
σc' = 5MPa
B.P. = 10MPa
T = 5℃
Sch= 32.7%
Sch= 44.9%
Smh= 35.1%
Smh= 41.9% (Hyodo et al. 2013)
Toyoura sand

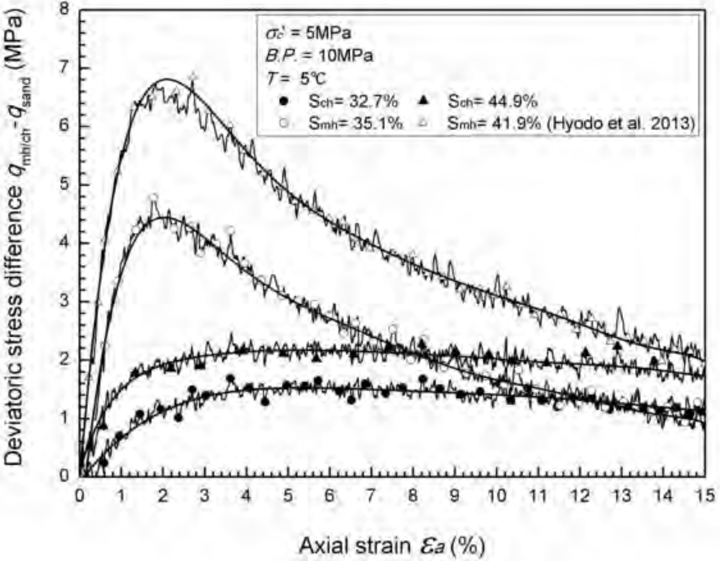

σc' = 5MPa
B.P. = 10MPa
T = 5℃
Sch= 32.7%
Sch= 44.9%
Smh= 35.1%
Smh= 41.9% (Hyodo et al. 2013)
Deviatoric stress difference q_mh/ch - q_sand (MPa)
Axial strain εa (%)
0
1
2
3
4
5
6
7
8
9
10
11
12
13
14
15

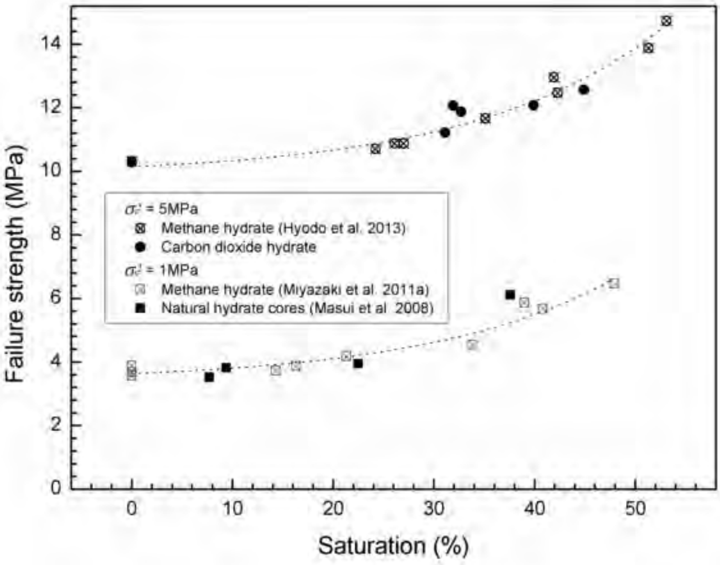

Failure strength (MPa)
Saturation (%)
σ₃' = 5MPa
Methane hydrate (Hyodo et al. 2013)
Carbon dioxide hydrate
σ₃' = 1MPa
Methane hydrate (Miyazaki et al. 2011a)
Natural hydrate cores (Masui et al. 2008)

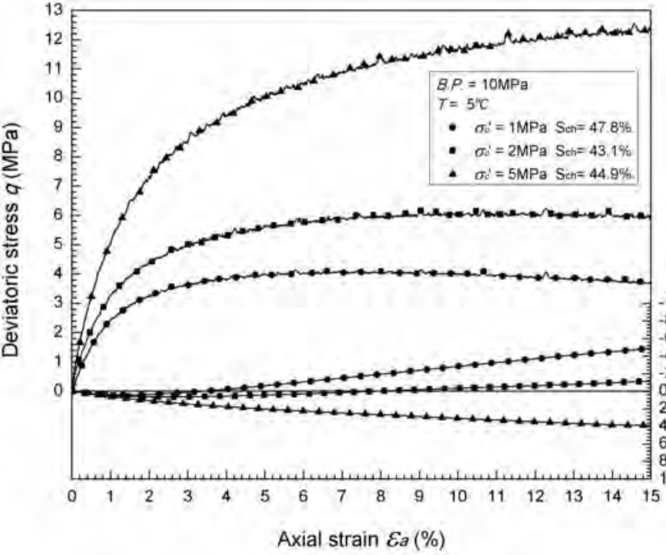

B.P. = 10MPa
T = 5℃
σc' = 1MPa Sch= 47.8%
σc' = 2MPa Sch= 43.1%
σc' = 5MPa Sch= 44.9%
Deviatoric stress q (MPa)
Volumetric strain εv (%)
Axial strain εa (%)

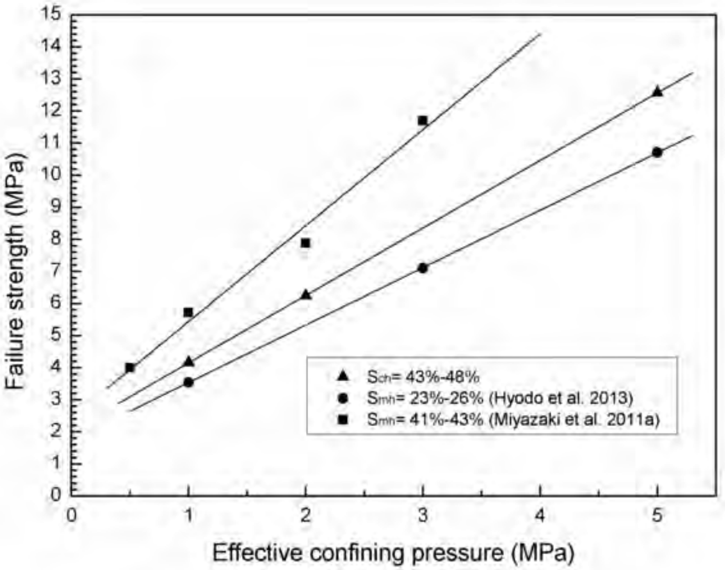

Failure strength (MPa)
Effective confining pressure (MPa)
0
1
2
3
4
5
6
7
8
9
10
11
12
13
14
15
0
1
2
3
4
5
Sch= 43%-48%
Smh= 23%-26% (Hyodo et al. 2013)
Smh= 41%-43% (Miyazaki et al. 2011a)

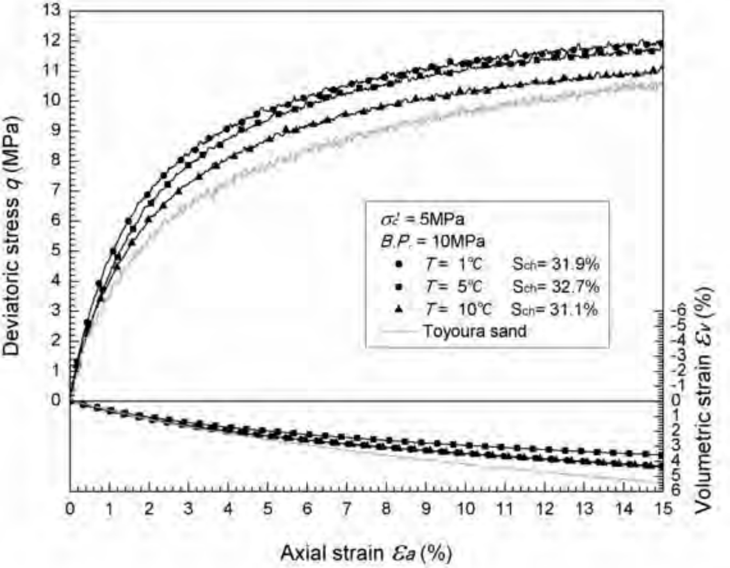

Deviatoric stress q (MPa)
Volumetric strain εv (%)
Axial strain εa (%)
σc' = 5MPa
B.P. = 10MPa
T = 1℃ Sch= 31.9%
T = 5℃ Sch= 32.7%
T = 10℃ Sch= 31.1%
Toyoura sand

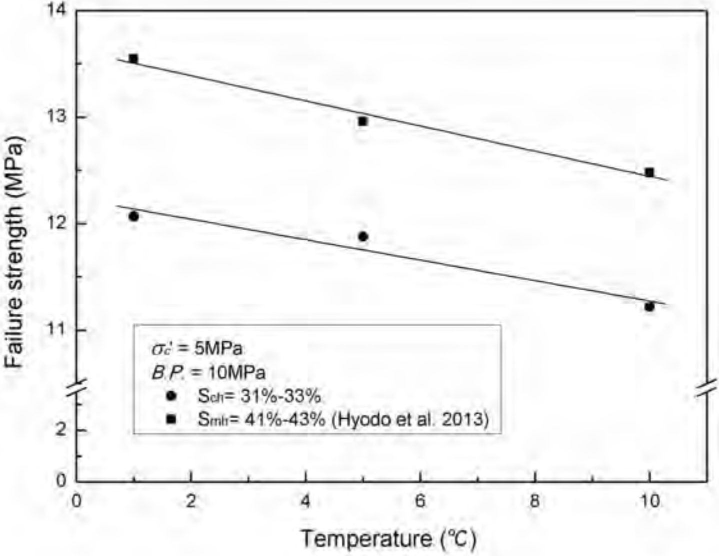

Failure strength (MPa)
Temperature (℃)
σc' = 5MPa
B.P. = 10MPa
Sch= 31%-33%
Smh= 41%-43% (Hyodo et al. 2013)
14
13
12
11
2
0
0
2
4
6
8
10

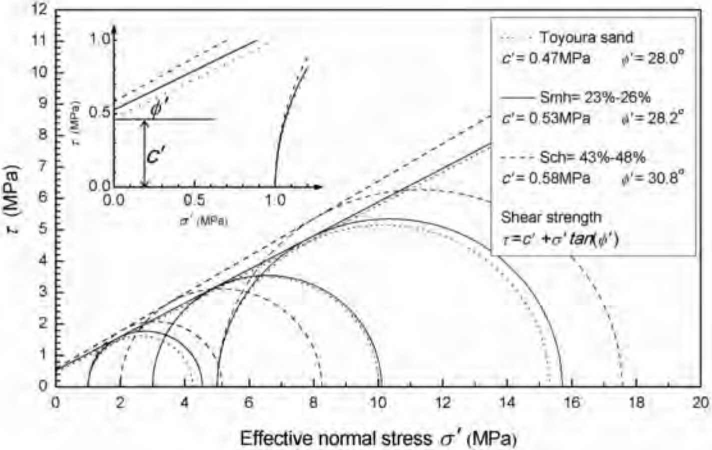
τ (MPa)
Effective normal stress σ' (MPa)
Toyoura sand
c' = 0.47MPa φ' = 28.0°
Smh= 23%-26%
c' = 0.53MPa φ' = 28.2°
Sch= 43%-48%
c' = 0.58MPa φ' = 30.8°
Shear strength
τ = c' + σ' tan(φ')
φ'
c'
τ (MPa)
σ' (MPa)

Table 1 Test conditions of triaxial compression tests

Test Conditions				Results
σ_c' (MPa)	*B.P.* (MPa)	T (℃)	S_{ch} (%)	q_{max} (MPa)
1	10	5	47.8	4.16
2	10	5	43.1	6.25
5	10	1	31.9	12.07
		5	0	10.32
			32.7	11.88
			39.9	12.08
			44.9	12.57
		10	31.1	11.22